Correlation functions and polaron-molecule crossover in one-dimensional attractive Fermi gases

Maolin Chang, Xiangguo Yin, and Li Chen
Institute of Theoretical Physics and State Key Laboratory of Quantum Optics and Quantum Optics Devices, Shanxi University, Taiyuan 030006, China

Yunbo Zhang*
Department of Physics and Key Laboratory of Optical Field Manipulation of Zhejiang Province, Zhejiang Sci-Tech University, Hangzhou 310018, China

(Received 31 January 2023; accepted 5 May 2023; published 18 May 2023)

We study the correlation functions in a one-dimensional attractive Fermi polaron system of spin-1/2 Fermi gas with one flipped spin as an impurity immersed in the fully polarized spin-up media. By means of the exact Bethe ansatz wave function with string solutions for the momentum, we manage to explicitly deduce the asymptotic form of the correlation functions in the infinite attractive limit and show that the system undergoes a polaron-molecule crossover when the attraction grows. The correlation functions in the infinite attractive limit can be decomposed into the free fermion term with the number of particles reduced by one and the molecular term indicated by the emergence of a sharp peak or dip in the central area of the correlation. These analytical results are checked by the numerical Monte Carlo methods for multiple integrals. The calculation is further extended to the excited states, i.e., the super-Tonks-Girardeau gas, and there is no peak or dip found in the vicinity of the correlation center. Tan contact is found to be proportional to the cubic of the interaction strength and the total energy is verified to satisfy the Tan adiabatic theorem in the strong attraction regime.

DOI: 10.1103/PhysRevA.107.053312

I. INTRODUCTION

In the past few decades, the ultracold Fermi gas has been used as a superb experimental platform for understanding many-body physics due to its high manipulability [1–4]. In particular, the experiments in a three-dimensional (3D) tunable Fermi liquid of ultracold atoms [5–7] give an opportunity to realize the Fermi polaron, a new form of quasi-particle induced by the mobile impurity, and the impurity systems attract more and more attention. Polarons are realized by means of atomic gases with population imbalance, the minority atoms playing the role of impurities while the majority one playing the role of background or medium. This system was realized experimentally with both bosonic [8–14] and fermionic [5,7,15,16] atoms. The experimental observation of nonequilibrium dynamics of a quantum impurity immersed in a bosonic environment [17] offers a systematic picture of polaron formation from weak to strong impurity interactions. A smooth polaron-molecule transition was observed in a spin-imbalanced ultracold Fermi gas with tunable interactions [18]. The Fermi polaron, on the other hand, could be attractive [5,16] or repulsive [7,15,19], which is a dressed spin-down impurity immersed in a polarized spin-up Fermi sea and the interaction between the impurity and the majority Fermi sea can be tuned precisely, from infinite repulsive to infinite attractive, with the help of Feshbach resonances [20].

However, most of the studies on the Fermi polaron problem, for example, the polaron-molecule transition in a 3D fermionic medium [16,21,22], are more or less involved with approximations based on variational methods or numerical techniques such as the renormalization group [23] or quantum Monte Carlo [24]. In contrast, many one-dimensional (1D) systems can be treated in exact ways, for instance, the Bethe ansatz, Bose-Fermi mapping, nonperturbative quantum field theory, and so on, which offers a test bench to understand the quasiparticle physics phenomena-like quantum criticality, quantum correlation, and so on. This model as a one-dimensional Fermi gas with Delta-function interaction was first treated by McGuire [25] for one flipped spin and later developed into the 1D many-body Fermi model by Yang [26] and Gaudin [27] in 1967. Using the Bethe ansatz hypothesis, 1D Fermi gases with arbitrary spin population imbalance are determined by a set of transcendental equations, which are known as the Bethe ansatz (BA) equations. In the unitary spin-1/2 Fermi gas close to the *s*-wave resonance various microscopic and thermodynamic properties depend universally on a key quality called the contact [28,29]. The analytical calculation with BA equations not only offers a benchmark to the 1D polaron problem, but also sheds light on exploring equilibrium and nonequilibrium many-body physics such as quantum phase transitions [30], Fulde-Ferrell-Larkin-Ovchinnikov (FFLO)-like pairing [31], and Tonks-Girardeau (TG) gases [32,33]. The time-dependent correlation functions of an impurity in 1D Fermi and Tonks-Girardeau gases with arbitrary temperature and arbitrary impurity-gas δ-function interactions were investigated in Fredholm determinant

*ybzhang@zstu.edu.cn

representation, which includes, as particular cases, the case for zero temperature and arbitrary repulsion, and for arbitrary temperature and infinite repulsion [34]. Recently a non-Gaussian state approach was developed to solve the ground-state and the out-of-equilibrium dynamics efficiently [35]. The variational approach showed that the polaron-molecule transition in the 3D fermion system can be reinterpreted as a first-order transition between single impurity systems with different total momenta [36]. These two states can coexist in a realistic system within a certain interaction window near their transition. It was further confirmed that the presence of a finite impurity concentration and low temperature directly lead to a smooth polaron-molecule transition as observed in recent experiments of 3D ultracold Fermi gases [18]. In one dimension, the system underwent a crossover from a mean-field polaron state into a mixture of excess fermions and a bosonic molecule as the attraction changed from weak to strong [37]. Finite concentration and low temperature would not change this picture and the polaron-molecule problem in one dimension was definitely a crossover. However, the asymptotic behavior of the correlation in the crossover between a polaron and molecule in one dimension still requires careful study.

At weak coupling, it is easy to find a good quantitative agreement with the experimental data. However, close to the Feshbach resonance the agreement becomes worse [18,38,39]. To understand the experimental data on RF spectroscopy and the Ramsey spectrum at finite temperature [19,40] it is essential to know the behavior of Fermi gases in the strongly interacting regime. In this work, we study the 1D Fermi polaron in the strongly attractive regime and provide an asymptotic form for the correlation functions. In the case of attractive interaction, there exist string solutions to the Bethe Ansatz equations, i.e., there is a pair of momentum always taking the imaginary values in the momentum set, which enables us to derive the analytical results of some important observables such as the correlation functions. However, one-body and density-density correlation functions show very different behaviors for weak and strong interaction and the impurity in the system tends to bind tightly to one of the background fermions, forming a molecule as the attraction grows. The system thus goes through a crossover between the polaron state and a mixture of one molecule and free fermions. Our analytical results are further checked by numerically calculating the correlation functions based on the Monte Carlo method.

The paper is organized as follows. In Sec. II we describe our model and write the wave function for one spin-down impurity explicitly. The one-body and density-density correlation functions are defined in Sec. III. We first illustrate the correlation of noninteracting free fermions in Sec. IV and present our key results in the strongly attractive limit in Sec. V. Furthermore, we obtain results for the excited states, i.e., the super-Tonks-Girardeau gas in Sec. VI. In comparison with other studies, Tan contact is also studied in the strong attraction limit in Sec. VII, which is closely related to the pair correlation function. We conclude our findings in Sec. VIII. The calculation details of the key integral are explained in the Appendix.

II. MODEL AND WAVE FUNCTION

We mainly focus on the system of one fermion with flipped spin immersed in a one-dimensional fully polarized Fermi gas, which is a special case of the famous Gaudin-Yang model [26,27] with the flipped spin serving as the single impurity. Its Hamiltonian takes the form

$$\mathcal{H} = \sum_{\sigma=\uparrow,\downarrow} \int dx \psi_\sigma^\dagger(x) \left(-\frac{\hbar^2}{2m} \frac{d^2}{dx^2} \right) \psi_\sigma(x) + \frac{g}{2} \int dx \psi_\uparrow^\dagger(x) \psi_\downarrow^\dagger(x) \psi_\downarrow(x) \psi_\uparrow(x), \tag{1}$$

where m is the atomic mass, $g = -2\hbar^2/ma_{1D}$ is the interaction strength between different spins, a_{1D} is the effective 1D scattering length, and the field operator $\psi_\sigma(x)$ [$\psi_\sigma^\dagger(x)$] annihilates (creates) a particle of spin σ at the spatial position x. For simplicity, we consider the system in a configuration of one spin-down and $N-1$ spin-up particles. By setting $c = mg/\hbar^2$, the Hamiltonian (1) can be reduced into the first quantization form

$$H = -\sum_{i=1}^{N} \frac{\partial^2}{\partial x_i^2} + 2c \sum_{i<j} \delta(x_i - x_j), \tag{2}$$

which describes N fermions via δ-function interaction in one dimension.

The model (2) was first solved by Gaudin [27] and Yang [26] in 1967. Due to the fact that the interaction only occurs when two fermions with opposite spins get in contact with each other, the wave function ψ can be divided into N different regions according to the relative position of the spin-down particle with respect to the background spin-up particles. For example, $x_N < x_1, x_2, \ldots, x_{N-1}$ is denoted as region 1, $x_i < x_N < x_1, x_2, \ldots, x_{i-1}, x_{i+1}, \ldots, x_{N-1}$ with $i = 1, 2, \ldots, N-1$ as region 2, and so on, where we label the coordinates of the spin-down particle as x_N. Following the Bethe ansatz, the wave function in each region can be expressed as the superposition of $N!$ plane waves, respectively. In region 1, for instance, the wave function is

$$\phi = \sum_P (-1)^P \alpha_N \prod_{n=1}^{N} e^{ik_{P_n} x_n}, \tag{3}$$

where $\alpha_N = 1 - e^{ik_N L}$ with L the length of the 1D system and P refers to any possible permutation of quasi-momentum $k's$. Using the periodic boundary condition $\psi(x_1, \ldots, x_i, \ldots, x_N) = \psi(x_1, \ldots, x_i + L, \ldots, x_N)$, the wave function in region i: $x_1, x_2, \ldots, x_{i-1} < x_N < x_i, \ldots, x_{N-1}$ can be expressed through the wave function in region 1 and the sum of all regions is equivalent to the wave function in the full region. Thus

$$\begin{aligned} &\psi(x_1, x_2, \ldots, x_N) \\ &= \Theta(x_N < x_1, \ldots, x_{N-1}) \phi(x_1, x_2, \ldots, x_N) \\ &\quad + \sum_{i=2}^{N} \Theta(x_1, \ldots, x_{i-1} < x_N < x_i, \ldots, x_{N-1}) \\ &\quad \times \phi(x_1 + L, x_2 + L, \ldots, x_{i-1} + L, x_i, \ldots, x_N), \end{aligned} \tag{4}$$

where the Heaviside step function $\Theta(x)$ is used to select the region wherein the wave function lies.

The quasi-momenta of the system are determined by the Bethe ansatz (BA) equations

$$\frac{k_n-\lambda+ic'}{k_n-\lambda-ic'}=e^{ik_nL}, \tag{5}$$

with $n=1,2,\ldots,N$ and

$$\prod_{n=1}^{N}\frac{k_n-\lambda+ic'}{k_n-\lambda-ic'}=1, \tag{6}$$

where $c'=c/2$ and λ is the rapidity. Utilizing these equations, we can obtain a general expression for the wave function in the full region

$$\psi(x_1,x_2,\ldots,x_N)=A\sum_P(-1)^P e^{ik_{P_N}x_N}\prod_{n=1}^{N-1}\left[k_{P_n}-\lambda+ic'\mathrm{sgn}(x_N-x_n)\right]e^{ik_{P_n}x_n}, \tag{7}$$

where $A=\frac{-2ic'}{\prod_{l=1}^{N}(k_l-\lambda-ic')}$. Note that here the influence of the region is absorbed into the sign function $\mathrm{sgn}(x_N-x_n)$. The wave function and BA equations are valid in the full interaction regime, either the repulsive or attractive one. For $c'=0$, the wave function naturally reduces to that of free fermions, which is described by the Slater determinant. BA equations yield the exact values of all momenta of free fermions as well. In this paper, we only focus on the case of the attractive interaction, i.e., $c'<0$, for which the roots of the BA equations k's contain a complex conjugate pair while the other $(N-2)$ are real. We assume the particle number N is even for simplicity.

III. CORRELATION FUNCTIONS

A. One-body correlation function

The one-body correlation function for the spin-up fermions is defined as the relative probability of creating a particle at position x while annihilating one with the same spin at x' simultaneously

$$\begin{aligned}g^{(1)}_{\uparrow\uparrow}(N,c';x,x')&=\langle a^\dagger_\uparrow(x)a_\uparrow(x')\rangle\\&=\frac{(N-1)L}{G}\int_0^L dx_2\cdots\int_0^L dx_N\\&\quad\times\psi^*(x,x_2,\ldots,x_N)\psi(x',x_2,\ldots,x_N),\end{aligned} \tag{8}$$

where

$$G=\int_0^L dx_1\cdots\int_0^L dx_N|\psi(x_1,x_2,\ldots,x_N)|^2 \tag{9}$$

is the normalization factor. The factor $N-1$ in Eq. (8) accounts for the fact that correlation for spin-up fermions actually occurs with $N-1$ possibilities, with x and x' replacing any one of the coordinates $x_1,x_2,\ldots,x_{N-1}$, respectively. Because of the conservation of spins, the one-body correlation function in different spin states, $g^{(1)}_{\uparrow\downarrow}(N,c';x,x')$, must vanish, which means one can not annihilate a fermion with spin-up and create one with spin-down.

B. Density-density correlation functions

The density-density correlation function between up spins is defined as

$$\begin{aligned}g^{(2)}_{\uparrow\uparrow}(N,c';x,x')&=\langle a^\dagger_\uparrow(x)a^\dagger_\uparrow(x')a_\uparrow(x')a_\uparrow(x)\rangle\\&=\langle a^\dagger_\uparrow(x)a_\uparrow(x)a^\dagger_\uparrow(x')a_\uparrow(x')\rangle-\delta(x-x')\langle a^\dagger_\uparrow(x)a_\uparrow(x')\rangle\\&=\frac{(N-1)(N-2)L^2}{G}\int_0^L dx_3\cdots\int_0^L dx_N\\&\quad\times\psi^*(x,x',x_3,\ldots,x_N)\psi(x,x',x_3,\ldots,x_N),\end{aligned} \tag{10}$$

and that between the opposite spins, also known as the pair correlation function [22], is given by

$$\begin{aligned}g^{(2)}_{\uparrow\downarrow}(N,c';x,x')&=\langle a^\dagger_\uparrow(x)a^\dagger_\downarrow(x')a_\downarrow(x')a_\uparrow(x)\rangle\\&=\langle a^\dagger_\uparrow(x)a_\uparrow(x)a^\dagger_\downarrow(x')a_\downarrow(x')\rangle\\&=\frac{(N-1)L^2}{G}\int_0^L dx_3\cdots\int_0^L dx_{N-1}\\&\quad\times\psi^*(x,x_2,\ldots,x_{N-1},x')\psi(x,x_2,\ldots,x_{N-1},x').\end{aligned} \tag{11}$$

Since there is only one impurity with opposite spin in the system, the density-density correlation between down spins vanishes, i.e., $g^{(2)}_{\downarrow\downarrow}(N,c';x,x')=0$. The factor $(N-1)(N-2)$ appears in Eq. (10) results from the fact that x and x' could replace any two coordinates in $x_1,x_2,\ldots,x_{N-1}$, leading to C^2_{N-1} possibilities. Due to the impurity being labeled as x_N, the coordinate x' for the spin-down fermion in the up-down correlation function (11) can only replace x_N, while the coordinate x for spin-up fermions can replace any one in $x_1,x_2,\ldots,x_{N-1}$, which contributes to the factor $N-1$ in Eq. (11). The density-density correlation functions represent the probability to find a spin-up fermion at x when there is a fermion with spin-up or spin-down at x'. We intentionally include two parameters, that is, the particle number N and interaction strength c', in the definition of the correlation function, as we shall see later the analytical results of the correlation function for different particle number and interaction strength are related to each other.

IV. GROUND STATE FOR FREE FERMIONS

We first consider the limit of the noninteracting case, i.e., the free fermion with $c'=0$. The analytical results in this limit were already obtained in [39]. The wave function of N free fermions is straightforwardly expressed as a superposition of plane waves

$$\psi(x_1,x_2,\ldots,x_N)=\sum_P(-1)^P e^{ik_Nx_N}\prod_{n=1}^{N-1}e^{ik_{P_n}x_n}, \tag{12}$$

which is consistent with our result (7) under condition $c'=0$, where the momentum of the spin-down fermion is denoted

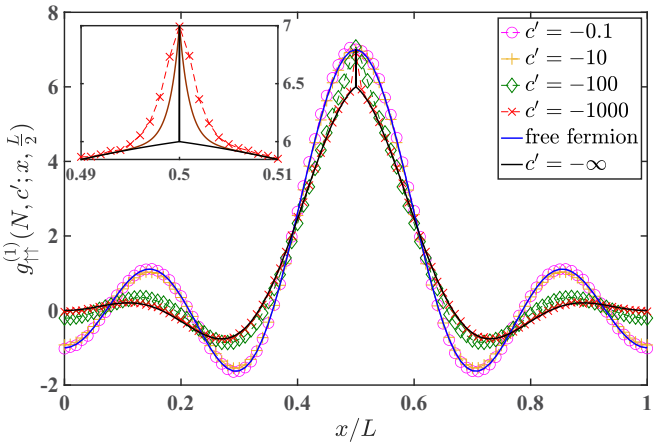

FIG. 1. One-body correlation functions for the ground states of $N = 8$ fermions with the interaction strength $c' = -0.1, -10, -100, -1000$, as well as the exact results for the free fermion gas and molecular state in the strong attraction limit $c' = -\infty$. The dashed lines with markers are numerical results from Monte Carlo integration methods, while the solid lines are analytical results. The inset shows the enlargement of the central peak, where the red dashed line is numerical result for $c' = -10^3$, the brown solid line and black solid line are analytical results for $c' = -10^3$ and -10^{10}, respectively. The unit of c' is L^{-1}.

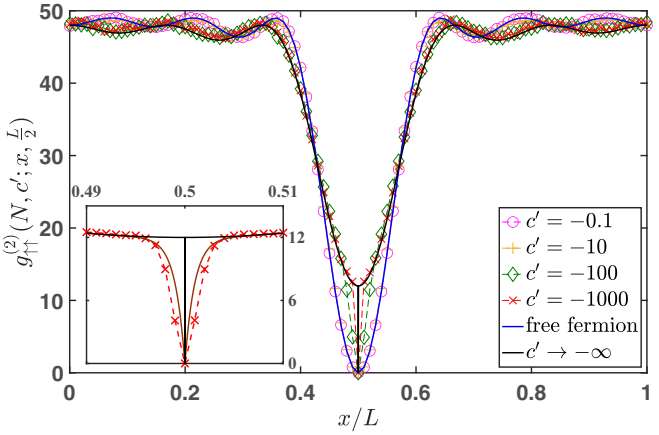

FIG. 2. Up-up correlation functions for the ground states of $N = 8$ fermions with the interaction strength $c' = -0.1, -10, -100, -1000$, as well as the exact results for free fermion gas and in the strong attraction limit. The dashed lines with markers are the Monte Carlo numerical results, while the solid lines are analytical results. The inset shows the enlargement of the central dip, where the red dashed lines are numerical result for $c' = -10^3$, the brown and black solid lines are analytical results for $c' = -10^3$ and -10^{10}, respectively. The unit of c' is L^{-1}.

as k_N. In this section, we present the calculation of one-body and density-density correlations of free fermions in the ground state, thus the momentum for spin-down fermion is $k_N = 0$. It is also easy to obtain the momentum values of other $N-1$ spin-up fermions from BA equations (5) and (6) due to the absence of interaction, i.e., $k_n = 0,\ \pm 2\pi/L,\ \pm 4\pi/L,\ \ldots,\ \pm(N-2)\pi/L$.

It is easy to calculate the one-body correlation function of N free fermions as

$$g^{(1)}_{\uparrow\uparrow}(N, 0; x, x') = \frac{\sin\left(\frac{(N-1)\pi}{L}(x'-x)\right)}{\sin\left(\frac{\pi}{L}(x'-x)\right)} \tag{13}$$

for spin-up fermions, which exhibits oscillation with the distance of the particles as shown in Fig. 1. The density-density correlation function between up spins reads as

$$g^{(2)}_{\uparrow\uparrow}(N, 0; x, x') = (N-1)^2 - \left(\frac{\sin\left(\frac{(N-1)\pi}{L}(x'-x)\right)}{\sin\left(\frac{\pi}{L}(x'-x)\right)}\right)^2, \tag{14}$$

which is shown in Fig. 2. The density-density correlations between up-down spins, on the other hand, gives the probability of finding a spin-up fermion at x while there is a spin-down one at x'. Due to the absence of interaction, the presence of a spin-down fermion does not affect the density of spin-up fermions. Thus this density-density correlation proves to be a constant, i.e.,

$$g^{(2)}_{\uparrow\downarrow}(N, 0; x, x') = N - 1. \tag{15}$$

V. GROUND STATE IN THE STRONGLY ATTRACTIVE LIMIT

Another topic of interest is the strongly attractive limit $c' \to -\infty$, the analytical results of which will serve as a benchmark for comparison in the attractive interaction regime, just as the free fermion case $c' \to 0$ is another limit in the study of the asymptotic behavior of correlation functions. As long as the attractive interaction is on, the BA equations (5) and (6) have solutions with complex quasi-momentum in addition to the real ones, which are purely imaginary for the ground state with periodic boundary conditions. This pair of complex momenta, known as string solutions, was first introduced in [41] so that the BA equations can be solved analytically for the attractive case of bosons.

In this section we present the calculation of ground-state correlation functions in the strong attraction limit $c' \to -\infty$. With the two-string solution assumption, a complex momentum pair $k_\pm = \pm ic'$ belongs to a pair of spin-up and spin-down particles even in the very strong attractive regime, i.e., two particles with opposite spins form a molecule due to the attraction and the BA equation (5) of the other $N-2$ real momentum can be derived as

$$e^{ik_n L} = -1 \tag{16}$$

since they are negligibly small compared to c'. Since the coordinate of the spin-down particle is labeled as x_N and its momentum can be either $k_N = k_+$ or k_-, the momentum of spin-up particles can be any permutation of the remaining $N-1$ momentum, i.e., $k_{Q_n} = \pm\pi/L, \pm 3\pi/L, \ldots, \pm(N-3)\pi/L$, k_- or k_+, where Q is the permutation of $N-1$ momentum and its elements depend on the value of k_N. Then the

wave function with spin-down particle located at x_N can be simplified as

$$\psi(x_1, x_2, \ldots, x_N) = \sum_{k_N=k_\pm} \sum_{Q} (-1)^Q (1 - e^{ik_N L}) e^{ik_N x_N} \prod_{n=1}^{N-1} e^{ik_{Q_n}[x_n + L\Theta(x_N - x_n)]} \tag{17}$$

from which the asymptotic behavior of the correlation functions are calculated.

A. One-body correlation function

Define $X_n = x_n + L\Theta(x_N - x_n)$, which means

$$X_n = \begin{cases} x_n + L, & x_n < x_N, \\ x_n, & x_n > x_N. \end{cases} \tag{18}$$

Inserting the exact Bethe ansatz wave function into the correlation function (8), we have

$$g^{(1)}_{\uparrow\uparrow}(N, c'; x, x') = \frac{(N-1)L}{G} I, \tag{19}$$

with the integral

$$I = \sum_{Q,Q'} \int_0^L dX_N \left(e^{ik_{Q_1} X}\right)^* e^{ik_{Q'_1} X'} A \times \prod_{n=2}^{N-1} \left(\int_{x_N}^{x_N + L} dX_n \left(e^{ik_{Q_n} X_n}\right)^* e^{ik_{Q'_n} X_n} \right). \tag{20}$$

Note that the factor $A = |(1 - e^{ik_N L}) e^{ik_N x_N}|^2$ is X_N dependent and X, X' are defined in similar way to X_n. We need take to into consideration the factor A, as k_N will determine the imaginary momentum in Q and Q'. The leading terms of A take the form of

$$A \approx \begin{cases} e^{-2c'L} e^{-2c' x_N}, & k_N = k_+, \\ e^{2c' x_N}, & k_N = k_-. \end{cases} \tag{21}$$

The integral is calculated step by step: first do the $(N-2)$-multiple integrals over $X_2, \ldots, X_{N-1}$, then extract the primary contribution in the integration of X_N, and finally do the summation over Q and Q'. It is shown that the leading-order contribution to the integral I up to $1/c'$ occurs when the permutations Q and Q' are identical (see the Appendix). The up-up one-body correlation function takes the following asymptotic behavior when $c' \to -\infty$:

$$g^{(1)}_{\uparrow\uparrow}(N, c'; x, x') = \left(1 - \frac{2|x' - x|}{L}\right) \frac{\sin\left(\frac{(N-2)\pi}{L}(x' - x)\right)}{\sin\left(\frac{\pi}{L}(x' - x)\right)} + e^{c'|x' - x|}. \tag{22}$$

The first term accounts for the case that the correlated particles at x and x' are not involved in the pairing with the impurity, such that the momenta k_{Q_1} and $k_{Q'_1}$ are real. The momentum of correlated particle, however, may indeed take imaginary values and we specifically calculate the corresponding contribution, i.e., the second term, which decays exponentially. In the summation over Q, the contribution of this term is negligibly small compared with the case of real k_{Q_1} in almost the entire space, except in the vicinity of the point $x' = x$. This means the up-spin particle paired with the impurity hardly contributes to the up-up correlation function or there is little possibility to annihilate one particle paired with the impurity and create it somewhere else, which is consistent with the constraint of infinite attraction.

In addition, according to our free fermion results (13), the correlation function (22) can be rewritten into the addition of two parts, i.e.,

$$g^{(1)}_{\uparrow\uparrow}(N, c'; x, x') = \left(1 - \frac{2|x' - x|}{L}\right) g^{(1)}_{\uparrow\uparrow}(N - 1, 0; x, x') + e^{c'|x' - x|}, \tag{23}$$

where $g^{(1)}_{\uparrow\uparrow}(N-1, 0; x, x')$ is exactly the one-body correlation function of $N-1$ free fermions. The second exponential term, on the other hand, vanishes in the entire range $0 \leqslant x < L$ except at $x = x'$, which represents a sharp peak in the correlation function in the vicinity of $x' = x$. It can be understood that in the limit of very strong attraction, the limit of $g^{(1)}_{\uparrow\uparrow}(N-1, 0; x, x')$ is $N-2$, while the limit of the second term is 1, resulting $g^{(1)}_{\uparrow\uparrow}(N, c'; x, x') = N - 1$ at $x = x'$. The inset of Fig. 1 demonstrates this behavior clearly as c' increases to very large negative values.

While BA equations can be solved analytically only for $c' = 0$ and in the limit of $c' \to -\infty$, we resort to the numerical approach to deal with the case of arbitrary intermediate interaction. We adopt the classical Monte Carlo (MC) method for standard calculation of the highly dimensional integral in the correlation functions (8), (10), and (11). As a powerful tool for high-dimensional integration, the MC method treats the numerical integral as a statistical average and obtains the averaged value by random sampling. This is exactly the problem we have to deal with as the particle number $N \gg 1$. Take the correlation function (8) as an example. Practically, we sample N_{MC} random points in the $N-1$-dimensional coordinate space $x_2, \ldots, x_N$, and obtain the integral by averaging the integrand on these points. Since the numerical error always scales as $1/\sqrt{N_{\mathrm{MC}}}$, N_{MC} determines the truncation error of the MC. Our practical calculations reveal that $N_{\mathrm{MC}} = 10^7$ can provide a sufficiently small error for $N = 8$ and $|c'| \leqslant 1000$, in which case the numerical results are in fairly good agreement with our analytical results. Nevertheless, further increasing $|c'|$ would exacerbate the singularity of the integrand near $x = x'$, preventing the MC from convergence within our computational capability.

The up-up correlation functions $g^{(1)}_{\uparrow\uparrow}(N = 8, c'; x, x' = L/2)$ for fixed $x' = L/2$ are shown in Fig. 1 for several interaction strengths from weak to strong $c' = -0.1, -10, -100, -1000$, in addition to the cases of the free fermion $c' = 0$ and the infinite attraction $c' = -\infty$. We compare the numerical result for $c' = -10^3$ with the analytical results (22) for $c' = -10^3$ and $c' = -10^{10}$ in the inset of Fig. 1, showing that the peak value of the correlation function is indeed $N - 1$. For the number of samples $N_{\mathrm{MC}} \propto 10^7$, the standard errors of the correlation functions are less than 0.1, which thus can be neglected compared to the symbol size in Fig. 1, as well as in the figures for other correlation functions. We see that in the weak attraction regime the

numerical results are quite similar to the free fermion gas, which implies the impurity is only dressed by the spin-up background as a polaron, and causes little influence on the behavior of fermions. However, for the strong attraction case the first term in $g^{(1)}_{\uparrow\uparrow}(N, c'; x, x')$ dominates, the correlation function is closely related to that of $N-1$ free fermions when x is far away from $x' = L/2$, in addition to a position-dependent amplitude factor. This reflects the fact that under strong attraction one spin-up fermion is bound tightly with the impurity forming a molecule, which has little contribution to the overall feature of correlation. Only in the central position $x' = L/2$ does a sharp peak emerge to conserve both the particle number and spin. The emergence of the central peak in the one-body correlation function can be treated as a symbol of the crossover from polaron-like nature into a mixture of one molecule with fermion media [37].

B. Density-density correlation functions

Now we turn to the density-density correlation functions. The density-density correlation between up spins takes a similar form to the one-body correlation as

$$g^{(2)}_{\uparrow\uparrow}(N, c'; x, x') = \frac{(N-1)(N-2)L^2}{G} J, \tag{24}$$

with the integral

$$J = \sum_{Q,Q'} \int_0^L dX_N \left(e^{ik_{Q_1}X} e^{ik_{Q_2}X'}\right)^* e^{ik_{Q'_1}X} e^{ik_{Q'_2}X'} A \times \prod_{n=3}^{N-1} \left(\int_{x_N}^{x_N+L} dX_n \left(e^{ik_{Q_n}X_n}\right)^* e^{ik_{Q'_n}X_n} \right). \tag{25}$$

Here the strategy is the same as in the calculation of integral I in the one-body correlation: the $N-3$ multiple integral is done over $X_3, \ldots, X_{N-1}$, while that of X_N needs to be treated separately as the factor A is X_N dependent. Remember we aim to extract the leading-order contribution only, which means in the strong attraction limit $c' \to -\infty$, the integral with different momentum permutation Q and Q' results in a higher order of $1/c'$, which can be ignored according to the discussion in the Appendix. This gives the calculation of density-density correlation functions as follows. The orthogonality of the plane waves for real momentum again assures that the leading-order contribution to the integral occurs for identical elements $Q_3, \ldots, Q_{N-1}$ in the permutations Q and Q'. There are, however, two possible arrangements for the first two elements in the permutations Q and Q', i.e., $Q'_1 = Q_1$, $Q'_2 = Q_2$ or $Q'_1 = Q_2$, $Q'_2 = Q_1$. The integral J is again classified into J_1 and J_2 according to whether there exists an imaginary value in k_{Q_1} and k_{Q_2}. Taking these two possibilities into consideration, the correlation function can be derived as

$$g^{(2)}_{\uparrow\uparrow}(N, c'; x, x') = N(N-2) - \frac{\sin\left(\frac{(N-2)\pi}{L}(x'-x)\right)}{\sin\left(\frac{\pi}{L}(x'-x)\right)} \times \left(\frac{\sin\left(\frac{(N-2)\pi}{L}(x'-x)\right)}{\sin\left(\frac{\pi}{L}(x'-x)\right)} + 2e^{c'|x'-x|} \right). \tag{26}$$

Similar to the one-body correlation function, we can decompose the above expression into the free fermion term and the molecular term

$$g^{(2)}_{\uparrow\uparrow}(N, c'; x, x') = g^{(2)}_{\uparrow\uparrow}(N-1, 0; x, x') + 2(N-2) - 2e^{c'|x'-x|} \frac{\sin\left(\frac{(N-2)\pi}{L}(x'-x)\right)}{\sin\left(\frac{\pi}{L}(x'-x)\right)}, \tag{27}$$

where the exponential term plays an important role only in the vicinity of $x' = x$. As shown in Fig. 2, the exact result of up-up correlation $g^{(2)}_{\uparrow\uparrow}(N = 8, c'; x, x' = L/2)$ for $c' = -10^3, -10^{10}$ exhibits a sharp dip at $x = L/2$, which is consistent with our numerical result for $c' = -10^3$. In the central position $x = L/2$ the density-density correlation approaches zero, while for being x away from $L/2$ the correlation behaves much like $N-1$ noninteracting fermions.

From the numerical results for several typical interaction strengths, we see that the density-density correlation between up-spins behaves like free fermions for weak attraction. With a spin-up particle already located at $x' = L/2$, the probability to find another one at the same position is zero due to the Pauli exclusion principle no matter if it is for the weak or strong interaction. The correlation function oscillates with distance and becomes stable slowly away from the correlated particle. In the strong attraction limit, a sharp dip emerges at $x = L/2$ while the correlation in the neighboring area is relatively low. Note that our analytical result (27) can be divided into two parts, the first line is the density-density correlation of $N-1$ fermions with no interaction with a constant shift by $2(N-2)$, and the second line contributes a dip at $x = L/2$ (note the minus sign), showing the distinct feature of the correlation between the fermions both in and outside the molecule.

The density-density correlation between opposite spins is evaluated alongside with the result

$$g^{(2)}_{\uparrow\downarrow}(N, c'; x, x') = g^{(2)}_{\uparrow\downarrow}(N-1, 0; x, x') - c'L(e^{2c'|x'-x|} + e^{2c'(L-|x'-x|)}). \tag{28}$$

The results of finite interaction are also calculated numerically, shown in Fig. 3. We see that a peak emerges immediately as the attraction turns on, which implies the spin-down impurity forming a polaron in the background of spin-up fermions. From the analytical result (28), the height of the peak is clearly proportional to $c'L$ when the interaction strength becomes large. It is easy to understand. Once the spin-down impurity is located at $x' = L/2$, it is highly possible to find a spin-up particle there due to the strong attractive interaction. As a result, the probability to find the spin-up particle elsewhere tends to be a constant. Physically, this signature indicates that the system experiences a crossover from a polaron-like behavior to a molecule state.

VI. EXCITED STATE: SUPER-TONKS-GIRARDEAU GAS

In this section, we study the correlation behavior of the excited states in the strong attraction limit. The energy spectrum in the full interaction regime can be calculated with the numerical solution of the BA equation. In the attractive

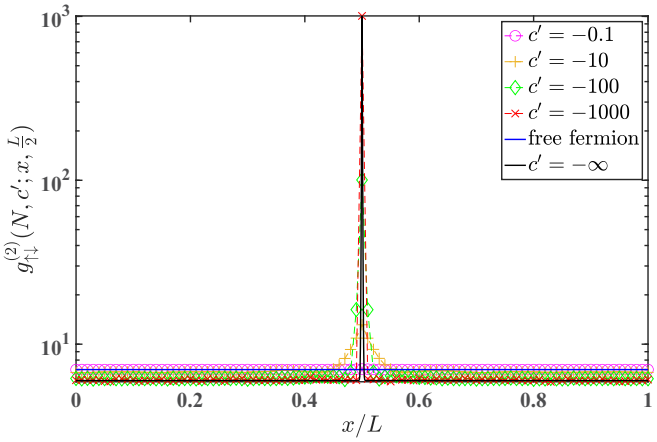

FIG. 3. Up-down correlation for the ground state of $N = 8$ fermions with the interaction strength $c' = -0.1$, -10, -100, -1000, the exact results for free fermion gas and in the strong attraction limit. The dashed line with markers are Monte Carlo numerical results, while the solid lines are analytical results. The unit of c' is L^{-1}.

regime ($-1/c' > 0$) the energy spectrum are clearly classified into two branches as shown in Fig. 4. The blue solid lines are shown for the gas states [42] in which all momentum k's are real and the minimum energy is positive. Such a state in the particular case $c' \to -\infty$ is known as the super-Tonks-Girardeau (STG) gas and was experimentally realized in bosonic cesium atoms [43] by suddenly switching the interaction from the strongly repulsive to attractive regime. The real ground state we studied in the previous section, however, belongs to the so-called bound states denoted by the red dashed lines (in fact, the lowest state, bold curve), which do not require real k's and only exist for the attractive interaction.

With the existence of the string solution, the correlation function of all bound states is quite similar to the ground state.

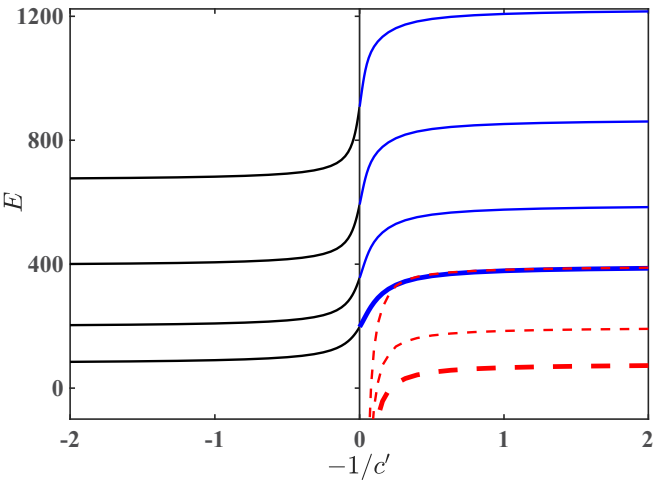

FIG. 4. The energy spectrum of $N = 4$ fermions with one impurity in the full interacting regime. The red lines are bound states while the blue ones refer to the gas states for attractive interaction. The black lines on the left ($-1/c' < 0$) are repulsive gas states. The STG gas refers to the many-body excited state for the particular case $c' \to -\infty$. The unit of E is $\hbar^2/2m$ and the unit of $-1/c'$ is L.

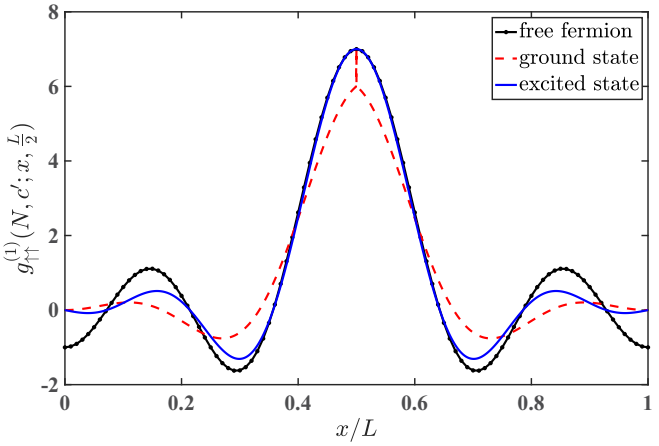

FIG. 5. Exact results of one-body correlation functions of $N = 8$ fermions for the free fermion gas, the ground state of strong attraction, and the excited STG gas state of strong attraction with minimum energy. For the ground state (red dashed line), the interaction strength c' is taken as -10^{10}. The unit of c' is L^{-1}.

On the other hand, in the STG gas state, the BA equation takes the same form as the bound states, i.e., Eq. (5), and can be simplified to $e^{ik_nL} = -1$ when $c' \to -\infty$. Since the solutions are all real, the momentum set for the lowest STG gas states (bold blue curve in Fig. 4) are $k_n = \pm\pi/L, \pm 3\pi/L, \ldots, \pm(N-1)\pi/L$. This similarity of the momentum set of the strong attractive gas state with that of free fermions makes the calculation of the one-body correlation function much easier and we obtain

$$g^{(1)}_{\uparrow\uparrow}(N, c'; x, x') = g^{(1)}_{\uparrow\uparrow}(N, 0; x, x') \cos\frac{\pi}{L}(x' - x). \tag{29}$$

The amplitude of the one-body correlation is modulated by a factor $\cos\frac{\pi}{L}(x' - x)$. The oscillation for the excited state is clearly suppressed in the entire 1D space. We compare the exact one-body correlation for the free fermion ground state, strongly attractive ground bound state, and the minimum energy STG gas in Fig. 5. Notice that in the STG state there is no peak in the vicinity of $x' = x$ as all momentum in the gas states are real and the correlation of gas states behaves more like the free fermion than the bound states.

For the same reason the up-up and up-down correlation functions in the STG gas can also be expressed with the help of free fermions and we find they are exactly identical

$$\begin{aligned} g^{(2)}_{\uparrow\uparrow}(N, c'; x, x') &= g^{(2)}_{\uparrow\uparrow}(N, 0; x, x'), \\ g^{(2)}_{\uparrow\downarrow}(N, c'; x, x') &= g^{(2)}_{\uparrow\downarrow}(N, 0; x, x') = N - 1. \end{aligned} \tag{30}$$

This means that the spin-up fermions experience a mean-field attraction as the impurity does not combine to form a molecule with any other particles. We compare the three up-up correlation functions in Fig. 6 and no dip is found in the vicinity of the correlation center.

VII. TAN CONTACT

The energy of the two-component Fermi gas with the s-wave contact interaction is a simple linear functional of its momentum distribution. This momentum distribution has a

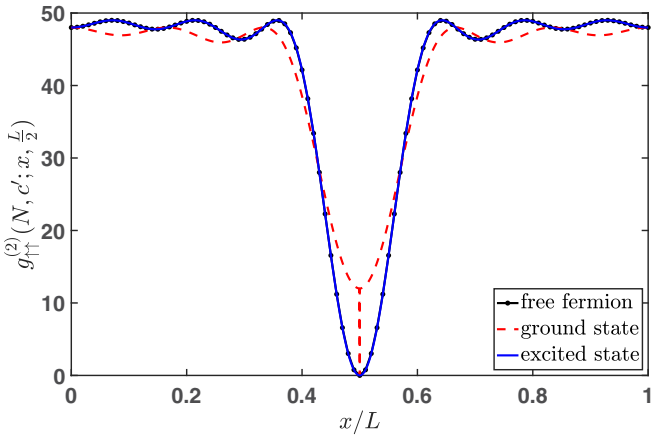

FIG. 6. Exact results of up-up correlation functions of $N = 8$ fermions for the free fermion gas, the ground state of strong attraction, and the excited STG gas state of strong attraction with minimum energy. For the ground state (red dashed line), the interaction strength c' is taken as -10^{10}. The unit of c' is L^{-1}.

tail proportional to $1/k^4$ at large k for large scattering length, the coefficient C of which is known as the Tan's contact [28]. For 1D systems, exact relations were derived to connect the universal C/k^4-decay of the momentum distribution at large k with the correlation functions. Specifically, the contact C is defined as an extensive variable, i.e., the integral of the probability density for two fermions with opposite spin to be at the same position in space and related to the pair correlation function as [44]

$$C = g^2 m^2 \int dx \langle a^\dagger_\uparrow(x) a^\dagger_\downarrow(x) a_\downarrow(x) a_\uparrow(x)\rangle = \frac{g^2 m^2}{L^2} \int dx g^{(2)}_{\uparrow\downarrow}(N, c'; x, x), \tag{31}$$

which is basically the expectation value of the interaction part of the Hamiltonian. The pair correlation function at short distances and the contact were calculated in the limit of infinite repulsion in Ref. [44]. Here we consider the limit of strong attraction, and find that the up-down spin correlation function is proportional to the interaction strength c' as

$$g^{(2)}_{\uparrow\downarrow}(N, c'; x, x) = -c' L, \tag{32}$$

which results in

$$C = -4\hbar^4 c'^3. \tag{33}$$

In the strong attraction regime, contact C is proportional to c'^3, which agrees with a previous study with numerical methods [45].

This extensive variable also determines the derivative of total energy E with respect to the 1D scattering length a_{1D}, which is known as the Tan adiabatic theorem [46]

$$\hbar^2 \frac{dE}{da_{1D}} = \frac{C}{2m}, \tag{34}$$

where $a_{1D} = -2\hbar^2/mg$. According to BA equations, the total energy E of the system depends on the summation of the momentum set k_n of all quasi-particles

$$E = \sum_n \frac{(\hbar k_n)^2}{2m} = \frac{\hbar^2}{2m}\left[\frac{2}{3}\left(\frac{\pi}{L}\right)^2 (4N^3 - 12N^2 + 11N - 3) - 2c'^2\right], \tag{35}$$

with $a_{1D} = -1/c'$, thus

$$\frac{dE}{da_{1D}} = c'^2 \frac{dE}{dc'} = -\frac{2\hbar^2}{m} c'^3 = \frac{C}{2m\hbar^2}, \tag{36}$$

which satisfies the Tan adiabatic theorem [44].

VIII. CONCLUSION

In conclusion, by means of the exact Bethe ansatz method, we studied the correlation function of 1D attractively interacting Fermions with one spin flipped, focusing on the crossover from polaron to molecule state with the increase of the interaction strength. We obtained exact analytical results for the correlation functions in the strong attraction limit. It showed that when the interaction strength $c' \to -\infty$, the correlation functions behaved very distinctly compared with the polaron in the weak attraction case, i.e., they all exhibited smooth oscillation in the 1D space when c' was small, while a sharp peak or dip emerged in the strong attraction limit. We numerically verified the calculation of the correlation functions in the full attraction regime with the help of the Monte Carlo method for multi-dimensional integration. These results confirmed that the system underwent a crossover from the polaron to the molecule state, and the emergence of the peak or dip characterized the crossover. We further studied the correlations in the excited STG states and found the crossover only occurs for the bound states with negative lowest energy. In addition, we provided the asymptotic behavior for the Tan's contact at short distances in the limit of infinite attraction. It was shown that some properties of the polaron depended on the range of the potential [47], and hence it should be interesting to further explore correlators of fermions with finite-range interaction.

ACKNOWLEDGMENTS

Y.Z. acknowledges support from the NSF of China (Grant No. 12074340) and the Science Foundation of Zhejiang Sci-Tech University (Grant No. 20062098-Y). L.C. acknowledges support from the NSF of China (Grants No. 12174236 and No. 12147215). X.Y. is supported by the NSF of Shanxi Province (Grant No. 202103021224033).

APPENDIX: CALCULATION OF THE INTEGRAL I

Here we show the calculation details of the integral I in Eq. (20) which can be rewritten as

$$I = \sum_{Q,Q'} \int_0^L dX_N \left(e^{ikQ_1 X}\right)^* e^{ikQ'_1 X'} A I', \tag{A1}$$

with

$$I' = \prod_{n=2}^{N-1} \left(\int_{x_N}^{x_N+L} dX_n \left(e^{ikQ_n X_n}\right)^* e^{ikQ'_n X_n} \right). \tag{A2}$$

The value of k_{Q_1} may be real or imaginary and the integral (A1) is classified into I_1 and I_2, respectively, such that $I = I_1 + I_2$.

First let us calculate I_1 by doing the $(N-2)$-multiple integral I' over X_n for $n = 2, 3, \ldots, N-1$. As $k_N = k_+$ or k_-, there is one and only one imaginary momentum in k_{Q_n}, as well as in $k_{Q'_n}$, taking the value of $-k_N$. For the integral over X_n, in most cases, we will meet the situation in which both momenta k_{Q_n} and $k_{Q'_n}$ are real; it is ready to use the orthogonality of the plane waves just as in the case of the free Fermi gas, i.e.,

$$\int_{x_N}^{x_N+L} \left(e^{ik_{Q_n}X_n}\right)^* e^{ik_{Q'_n}X_n} dX_n = L\delta_{Q_nQ'_n}. \tag{A3}$$

The imaginary momentum, however, may appear either at different positions in the permutation Q and Q' (Case A), and thereafter one of them is the real momentum and the other imaginary, or at the same positions (Case B), in which case both k_{Q_n} and $k_{Q'_n}$ are purely imaginary in the integral. The integral is then calculated for these two cases, respectively.

Case A. When one of them, say k_{Q_n}, is imaginary, and $k_{Q'_n}$ is real, the key step here is to calculate the integral of the string solution. The leading-order contribution to the integral over X_n proves to be

$$\int_{x_N}^{x_N+L} (e^{ik_+X_n})^* e^{ik_{Q'_n}X_n} dX_n \approx -\frac{1}{c'} e^{-c'(x_N+L)} \tag{A4}$$

for $k_{Q_n} = k_+$ and

$$\int_{x_N}^{x_N+L} (e^{ik_-X_n})^* e^{ik_{Q'_n}X_n} dX_n \approx -\frac{1}{c'} e^{c'x_N} \tag{A5}$$

for $k_{Q_n} = k_-$, where we use $e^{c'L} \to 0$ as c' is large and negative.

We adopt $(L-4)$ times the orthogonality relation (A3) and twice the Case A integrals (A4) or (A5) for X_n and $X_{n'}$ in the integral I', which gives

$$I' = L^{N-4} \int_{x_N}^{x_N+L} (e^{ik_\pm X_n})^* e^{ik_{Q'_n}X_n} dX_n \times \int_{x_N}^{x_N+L} \left(e^{ik_{Q_{n'}}X_{n'}}\right)^* e^{ik_\pm X_{n'}} dX_{n'}. \tag{A6}$$

For $k_N = k_+$, we know $k_{Q_n} = k_{Q'_{n'}} = k_-$, thus

$$AI' \approx e^{-2c'L} e^{-2c'x_N} L^{N-4} \left(-\frac{1}{c'} e^{c'x_N}\right)^2 = \frac{L^{N-4}}{c'^2} e^{-2c'L}, \tag{A7}$$

otherwise for $k_N = k_-$, we have $k_{Q_n} = k_{Q'_{n'}} = k_+$, and

$$AI' \approx e^{2c'x_N} L^{N-4} \left(\frac{1}{-c'} e^{-c'(x_N+L)}\right)^2 = \frac{L^{N-4}}{c'^2} e^{-2c'L}. \tag{A8}$$

Clearly we arrive at the same result AI' for either $k_N = k_+$ or $k_N = k_-$.

Case B. When both k_{Q_n} and $k_{Q'_n}$ are purely imaginary, the integral of X_n becomes

$$\int_{x_N}^{x_N+L} (e^{ik_+X_n})^* e^{ik_+X_n} dX_n \approx -\frac{1}{2c'} e^{-2c'(x_N+L)} \tag{A9}$$

for $k_{Q_n} = k_{Q'_n} = k_+$ and

$$\int_{x_N}^{x_N+L} (e^{ik_-X_n})^* e^{ik_-X_n} dX_n \approx -\frac{1}{2c'} e^{2c'x_N} \tag{A10}$$

for $k_{Q_n} = k_{Q'_n} = k_-$.

We adopt $(L-3)$ times the orthogonality relation (A3) and once the Case B integral (A9) or (A10) for X_n in the integral I', which gives

$$I' = L^{N-3} \int_{x_N}^{x_N+L} (e^{ik_\pm X_n})^* e^{ik_\pm X_n} dX_n. \tag{A11}$$

For $k_N = k_+$, we know $k_{Q_n} = k_{Q'_n} = k_-$, thus

$$AI' \approx e^{-2c'L} e^{-2c'x_N} L^{N-3} \frac{1}{-2c'} e^{2c'x_N} = -\frac{L^{N-3}}{2c'} e^{-2c'L}, \tag{A12}$$

otherwise for $k_N = k_-$, we have $k_{Q_n} = k_{Q'_n} = k_+$, and

$$AI' \approx e^{2c'x_N} L^{N-3} \frac{1}{-2c'} e^{-2c'(x_N+L)} = -\frac{L^{N-3}}{2c'} e^{-2c'L}. \tag{A13}$$

Again we arrive the same result AI' for either $k_N = k_+$ or $k_N = k_-$.

We see that the leading-order terms in AI' are independent of X_N, and Case A is of order $1/c'^2$ while Case B is $1/c'$ besides the exponential factor $e^{-2c'L}$. It is thus justified to omit the contribution from case A.

The next step is the integral of X_N. Inserting back the definition of X and X', we find

$$\int_0^L \left(e^{ik_{Q_1}X}\right)^* e^{ik_{Q'_1}X'} dX_N = \left(e^{ik_{Q_1}x}\right)^* e^{ik_{Q'_1}x'} I_N, \tag{A14}$$

where the integration I_N can be split into three regions: $(0, x)$, (x, x'), and (x', L) for $x < x'$ and the step functions only take values in the middle region

$$I_N = \int_0^L e^{ik_{Q_1}L[\Theta(x_N-x')-\Theta(x_N-x)]} dx_N = \int_0^x e^0 dx_N + \int_x^{x'} e^{-ik_{Q_1}L} dx_N + \int_{x'}^L e^0 dx_N = L - 2(x'-x). \tag{A15}$$

Notice that k_{Q_1} is real and can only take values of odd multiples of π/L. For $x > x'$, we simply interchange x and x'. We thus have

$$\int_0^L \left(e^{ik_{Q_1}X}\right)^* e^{ik_{Q'_1}X'} dX_N = \left(e^{ik_{Q_1}x}\right)^* e^{ik_{Q'_1}x'} (L - 2|x'-x|). \tag{A16}$$

Keeping the leading-order terms in Case B means that in the summation $\sum_{Q,Q'}$ we only need to take into account the case when the two imaginary momenta occur at the same position, i.e., $k_{Q_n} = k_{Q'_n}$. Together with the orthogonality (A3) for real momentum, this simplifies the summation into $\sum_Q$, i.e., $Q = Q'$. The integral I_1 is now

$$I_1 = -\frac{L^{N-2}}{c'} e^{-2c'L}\Big(1 - \frac{2|x'-x|}{L}\Big)\sum_Q e^{ik_{Q_1}(x'-x)}. \quad \text{(A17)}$$

Now we do the summation of Q. Note that the sum of $Q_2, \ldots, Q_{N-1}$ results in a factor $(N-2)!$ and that of all real k_{Q_1} gives

$$\sum_{Q_1=1}^{N-2} e^{ik_{Q_1}(x'-x)} = \frac{\sin\left(\frac{(N-2)\pi}{L}(x'-x)\right)}{\sin\left(\frac{\pi}{L}(x'-x)\right)}. \quad \text{(A18)}$$

The final result for I_1 is

$$I_1 = -(N-2)!\frac{L^{N-2}}{c'}e^{-2c'L} \times \left(1 - \frac{2|x'-x|}{L}\right)\frac{\sin\left(\frac{(N-2)\pi}{L}(x'-x)\right)}{\sin\left(\frac{\pi}{L}(x'-x)\right)}. \quad \text{(A19)}$$

Now we calculate I_2 when k_{Q_1} is imaginary. In this case all other k_{Q_n} with $n = 2, \ldots, N-1$ are real, and by means of the orthogonality (A3) and the leading-order terms in A, it is shown that

$$I_2 = (N-2)!\sum_{Q_1}\int_0^L dX_N e^{ik_{Q_1}(X+X')}AL^{N-2}, \quad \text{(A20)}$$

where the terms from Case A are omitted just as before. For $k_N = k_+, k_{Q_1} = k_-$, the integral for X_N

$$L^{N-2}e^{-2c'L}\int_0^L e^{-2c'x_N}e^{c'(X+X')}dx_N \quad \text{(A21)}$$

is again split into three regions for $x < x'$

$$L^{N-2}e^{-2c'L}e^{c'(x+x')}\Big[\int_0^x e^{-2c'x_N}dx_N + e^{c'L}\int_x^{x'} e^{-2c'x_N}dx_N + e^{2c'L}\int_{x'}^L e^{-2c'x_N}dx_N\Big] \quad \text{(A22)}$$

with a quite simple result as

$$L^{N-2}e^{-2c'L}e^{c'(x+x')}\frac{1}{-2c'}[(e^{-2c'x}-1) + e^{c'L}(e^{-2c'x'}-e^{-2c'x}) + e^{2c'L}(e^{-2c'L}-e^{-2c'x'})] \approx -\frac{L^{N-2}}{2c'}e^{-2c'L}e^{c'(x'-x)}. \quad \text{(A23)}$$

Note that the step functions here gives 0, 1, 2 in the three regions due to the addition $(X + X')$ in the exponential function and among the six terms the first one proves to be the leading term. Similarly, for $k_N = k_-$, $k_{Q_1} = k_+$, we get exactly the same result. For $x > x'$, we again simply interchange x and x'. The combination of these results gives

$$I_2 = -(N-2)!\frac{L^{N-2}}{c'}e^{-2c'L}e^{c'|x'-x|}. \quad \text{(A24)}$$

Following the same procedure, the normalization factor G can be evaluated to the leading order as

$$G = -(N-1)!\frac{L^{N-1}}{c'}e^{-2c'L}. \quad \text{(A25)}$$

By collecting the integral I, i.e., the sum of Eqs. (A19) and (A24) and the normalization factor G into the expression of the up-up correlation function (19), we see that all terms are canceled perfectly, leading to the result of the up-up correlation function (22) in the main text.

[1] I. Bloch, J. Dalibard, and W. Zwerger, Many-body physics with ultracold gases, Rev. Mod. Phys. **80**, 885 (2008).

[2] S. Giorgini, L. P. Pitaevskii, and S. Stringari, Theory of ultracold atomic Fermi gases, Rev. Mod. Phys. **80**, 1215 (2008).

[3] X.-W. Guan, M. T. Batchelor, and C.-H. Lee, Fermi gases in one dimension: From Bethe ansatz to experiments, Rev. Mod. Phys. **85**, 1633 (2013).

[4] X.-W. Guan and P. He, New trends in quantum integrability: recent experiments with ultracold atoms, Rep. Prog. Phys. **85**, 114001 (2022).

[5] A. Schirotzek, C.-H. Wu, A. Sommer, and M. W. Zwierlein, Observation of Fermi Polarons in a Tunable Fermi Liquid of Ultracold Atoms, Phys. Rev. Lett. **102**, 230402 (2009).

[6] N. Navon, S. Nascimbène, F. Chevy, and C. Salomon, The equation of state of a low-temperature fermi gas with tunable interactions, Science **328**, 729 (2010).

[7] C. Kohstall, M. Zaccanti, M. Jag, A. Trenkwalder, P. Massignan, G. M. Bruun, F. Schreck, and R. Grimm, Metastability and coherence of repulsive polarons in a strongly interacting Fermi mixture, Nature (London) **485**, 615 (2012).

[8] J. Catani, G. Lamporesi, D. Naik, M. Gring, M. Inguscio, F. Minardi, A. Kantian, and T. Giamarchi, Quantum dynamics of impurities in a one-dimensional Bose gas, Phys. Rev. A **85**, 023623 (2012).

[9] N. Spethmann, F. Kindermann, S. John, C. Weber, D. Meschede, and A. Widera, Dynamics of Single Neutral Impurity Atoms Immersed in an Ultracold Gas, Phys. Rev. Lett. **109**, 235301 (2012).

[10] A. Shashi, F. Grusdt, D. A. Abanin, and E. Demler, Radio-frequency spectroscopy of polarons in ultracold Bose gases, Phys. Rev. A **89**, 053617 (2014).

[11] Y. E. Shchadilova, R. Schmidt, F. Grusdt, and E. Demler, Quantum Dynamics of Ultracold Bose Polarons, Phys. Rev. Lett. **117**, 113002 (2016).

[12] K. K. Nielsen, L. A. P. Ardila, G. M. Bruun, and T. Pohl, Critical slowdown of non-equilibrium polaron dynamics, New J. Phys. **21**, 043014 (2019).

[13] S. I. Mistakidis, G. C. Katsimiga, G. M. Koutentakis, T. Busch, and P. Schmelcher, Quench Dynamics and Orthogonality Catastrophe of Bose Polarons, Phys. Rev. Lett. **122**, 183001 (2019).

[14] M. Drescher, M. Salmhofer, and T. Enss, Theory of a resonantly interacting impurity in a Bose–Einstein condensate, Phys. Rev. Res. **2**, 032011(R) (2020).

[15] M. Koschorreck, D. Pertot, E. Vogt, B. Fröhlich, M. Feld, and M. Köhl, Attractive and repulsive Fermi polarons in two dimensions, Nature (London) **485**, 619 (2012).

[16] S. Nascimbène, N. Navon, K.-J. Jiang, L. Tarruell, M. Teichmann, J. McKeever, F. Chevy, and C. Salomon, Collective Oscillations of an Imbalanced Fermi Gas: Axial Compression Modes and Polaron Effective Mass, Phys. Rev. Lett. **103**, 170402 (2009).

[17] M. G. Skou, T. G. Skov, N. B. Jørgensen *et al.*, Non-equilibrium quantum dynamics and formation of the Bose polaron, Nat. Phys. **17**, 731 (2021).

[18] G. Ness, C. Shkedrov, Y. Florshaim, O. K. Diessel, J. von Milczewski, R. Schmidt, and Y. Sagi, Observation of a Smooth Polaron-Molecule Transition in a Degenerate Fermi Gas, Phys. Rev. X **10**, 041019 (2020).

[19] F. Scazza, G. Valtolina, P. Massignan, A. Recati, A. Amico, A. Burchianti, C. Fort, M. Inguscio, M. Zaccanti, and G. Roati, Repulsive Fermi Polarons in a Resonant Mixture of Ultracold ^{6}Li Atoms, Phys. Rev. Lett. **118**, 083602 (2017).

[20] C. Chin, R. Grimm, P. Julienne, and E. Tiesinga, Feshbach resonances in ultracold gases, Feshbach resonances in ultracold gases, Rev. Mod. Phys. **82**, 1225 (2010).

[21] G. M. Bruun and P. Massignan, Decay of Polarons and Molecules in a Strongly Polarized Fermi Gas, Phys. Rev. Lett. **105**, 020403 (2010).

[22] W. Li and X. Cui, Repulsive Fermi polarons with negative effective mass, Phys. Rev. A **96**, 053609 (2017).

[23] R. Schmidt and T. Enss, Excitation spectra and rf response near the polaron-to-molecule transition from the functional renormalization group, Phys. Rev. A **83**, 063620 (2011).

[24] N. Prokof'ev and B. Svistunov, Fermi-polaron problem: Diagrammatic Monte Carlo method for divergent sign-alternating series, Phys. Rev. B **77**, 020408(R) (2008).

[25] J. B. McGuire, Interacting Fermions in one dimension. I. Repulsive potential, J. Math. Phys. **6**, 432 (1965); Interacting Fermions in one dimension. II. Attractive potential, **7**, 123 (1966).

[26] C. N. Yang, Some Exact Results for the Many-Body Problem in one Dimension with Repulsive Delta-Function Interaction, Phys. Rev. Lett. **19**, 1312 (1967).

[27] M. Gaudin, Un systeme a une dimension de fermions en interaction, Phys. Lett. A **24**, 55 (1967).

[28] S. Tan, Energetics of a strongly correlated Fermi gas, Ann. Phys. (NY) **323**, 2952 (2008).

[29] S. Zhang and A. J. Leggett, Universal properties of the ultracold Fermi gas, Phys. Rev. A **79**, 023601 (2009).

[30] X.-W. Guan and T.-L. Ho, Quantum criticality of a one-dimensional attractive Fermi gas, Phys. Rev. A **84**, 023616 (2011).

[31] P. Fulde and R. A. Ferrell, Superconductivity in a strong spin-exchange field, Phys. Rev. **135**, A550 (1964).

[32] B. Paredes, A. Widera, V. Murg, O. Mandel, S. Fölling, I. Cirac, G. V. Shlyapnikov, T. W. Hänsch, and I. Bloch, Tonks-Girardeau gas of ultracold atoms in an optical lattice, Nature (London) **429**, 277 (2004).

[33] T. Kinoshita, T. Wenger, and D. S. Weiss, Observation of a one-dimensional Tonks-Girardeau gas, Science **305**, 1125 (2004).

[34] O. Gamayun, A. G. Pronko, and M. B. Zvonarev, Time and temperature-dependent correlation function of an impurity in one-dimensional Fermi and Tonks–Girardeau gases as a Fredholm determinant, New J. Phys. **18**, 045005 (2016).

[35] P. E. Dolgirev, Y.-F. Qu, M. B. Zvonarev, T. Shi, and E. Demler, Emergence of a Sharp Quantum Collective Mode in a One-Dimensional Fermi Polaron, Phys. Rev. X **11**, 041015 (2021).

[36] X. Cui, Fermi polaron revisited: Polaron-molecule transition and coexistence, Phys. Rev. A **102**, 061301(R) (2020).

[37] X.-W. Guan, Polaron, molecule and pairing in one-dimensional spin-1/2 Fermi gas with an attractive Delta-function interaction, Front. Phys. **7**, 8 (2012).

[38] H. Hu and X.-J. Liu, Raman spectroscopy of Fermi polarons, Phys. Rev. A **106**, 063306 (2022).

[39] R. Mao, X.-W. Guan, and B. Wu, Exact results for polaron and molecule in one-dimensional spin-1/2 Fermi gas, Phys. Rev. A **94**, 043645 (2016).

[40] Z. Yan, P. B. Patel, B. Mukherjee, R. J. Fletcher, J. Struck, and M. W. Zwierlein, Boiling a Unitary Fermi Liquid, Phys. Rev. Lett. **122**, 093401 (2019).

[41] M. Takahashi, *Thermodynamics of One-Dimensional Solvable Models* (Cambridge University Press, Cambridge, England, 1999).

[42] O. Gamayun, O. Lychkovskiy, and M. B. Zvonarev, Zero temperature momentum distribution of an impurity in a polaron state of one-dimensional Fermi and Tonks-Girardeau gases, SciPost Phys. **8**, 053 (2020).

[43] E. Haller, M. Gustavsson, M. J. Mark, J. G. Danzl, R. Hart, G. Pupillo, and H.-C. Nagerl, Realization of an excited, strongly correlated quantum gas phase, Science **325**, 1224 (2009).

[44] M. Barth and W. Zwerger, Tan relations in one dimension, Ann. Phys. **326**, 2544 (2011).

[45] Y. Song and X.-M. Cai, Properties of one-dimensional highly polarized fermi gases, Chin. Phys. Lett. **35**, 110301 (2018).

[46] S. Tan, Large momentum part of a strongly correlated Fermi gas, Ann. Phys. (NY) **323**, 2971 (2008).

[47] R. Pessoa, S. A. Vitiello, and L. A. P. Ardila, Finite-range effects in the unitary Fermi polaron, Phys. Rev. A **104**, 043313 (2021).